Geophys. J. Int. (2004) **157,** 354–362 doi: 10.1111/j.1365-246X.2004.02206.x

Insights into rifting from shear wave splitting and receiver functions: an example from Ethiopia

Atalay Ayele,[1] Graham Stuart[2] and J.-Michael Kendall[2]

[1] *Geophysical Observatory, Addis Ababa University, Addis Ababa, Ethiopia*
[2] *School of Earth Sciences, University of Leeds, Leeds* LS2 9JT*, UK. E-mail: graham@earth.leeds.ac.uk*

Accepted 2003 December 1. Received 2003 November 20; in original form 2003 February 3

SUMMARY

Seismic anisotropy beneath broad-band stations in the vicinity of the East African rift are compared with those on stable cratonic parts of Africa and Arabia. Such measurements offer potential constraints on rift processes, absolute plate motions (APM) and tectonic structure. New *SKS* shear wave splitting parameters are analysed beneath the broad-band stations of FURI and AAE (Ethiopia), BGCA (Central African Republic) and RAYN (Saudi Arabia). The number of events considered at the four stations varies from 13 to 32 and provides good azimuthal coverage. Stations on or near the rift show the polarization of the fast shear wave (ϕ) aligned parallel to the rift axis. The magnitude of the splitting delay (δt) increases northward along the East African rift. Previously published measurements in Kenya show the smallest splitting value (1.0 s), whilst the Djibouti station, ATD, shows the largest splitting (1.6 s). The Ethiopian results ($\delta t = 1.38 + 0.03$ s, $\phi = 36^\circ + 1$) show constancy in δt and ϕ with respect to backazimuth, thus, suggesting a single anisotropic layer beneath the stations. There is no observed correlation of ϕ with APM direction. Less splitting (δt) is observed beneath cratonic parts of Africa. BGCA in central Africa shows splitting parallel to the inferred direction of transpression, not the APM direction. Receiver-function analysis at FURI and AAE supports evidence from refraction experiments of thick crust (*ca* 40 km) in the region of continental rifting, however, the analysis shows a deeper interface at a depth of 90 km, also. This interface may mark the base of the lithosphere in this region. One interpretation of the splitting results is that the anisotropy at the Ethiopian stations is the result of aligned melt in this upper 90 km of lithosphere. $A < 1$ per cent volume fraction of melt aligned in thin (aspect-ratio <0.03) vertical ellipsoidal pockets generates sufficient splitting to explain the data. Higher splitting magnitudes in the north correlates with higher melt production observed in the Ethiopian part of the rift. Alternatively, anisotropy may be the result of the alignment of olivine in the asthenosphere parallel to the ridge axis, as material flows laterally to fill the gap caused by lithospheric extension. This would either suggest a northward-thickening anisotropic layer beneath the rift or enhanced olivine alignment as a result of changes in strain. Whatever the mechanism, it appears that the anisotropy is sensitive to, and provides insight into, the transition from continental to oceanic rifting in the northern Ethiopian rift.

Key words: Africa, anisotropy, melt, receiver functions, rifts, shear wave splitting.

1 INTRODUCTION

The African continent comprises different tectonic domains with a large contrast in age from the stable cratons to the now active Cenozoic East African rift system (EARS). We compare seismic anisotropy beneath broad-band stations in the vicinity of the East African rift (EAR) with those on the stable cratonic parts of Africa and Arabia (Fig. 1) in an attempt to assess whether the rift processes absolute plate motions (APM) or the tectonic structures provide the major control on deformation processes in the crust and upper mantle of the East African rift.

Seismic anisotropy of the mantle is generally thought to arise from strain-induced preferred orientation of highly anisotropic crystals such as olivine (Nicolas & Christensen 1987). There has been a gradual consensus that most of the anisotropy is concentrated in the upper mantle (Cara & Leveque 1988; Savage 1999; Silver & Chan 1991; Fischer & Wiens 1996; Friederich & Huang 1996). However, there is debate as to what extent this anisotropy is fossil anisotropy from past deformation (e.g. Archean) events (Silver 1996; Silver & Chan 1991) or a recent feature related to the current deformation of the lithosphere by upwelling mantle and asthenospheric flow (Vinnik *et al.* 1995; Fischer & Wiens 1996).

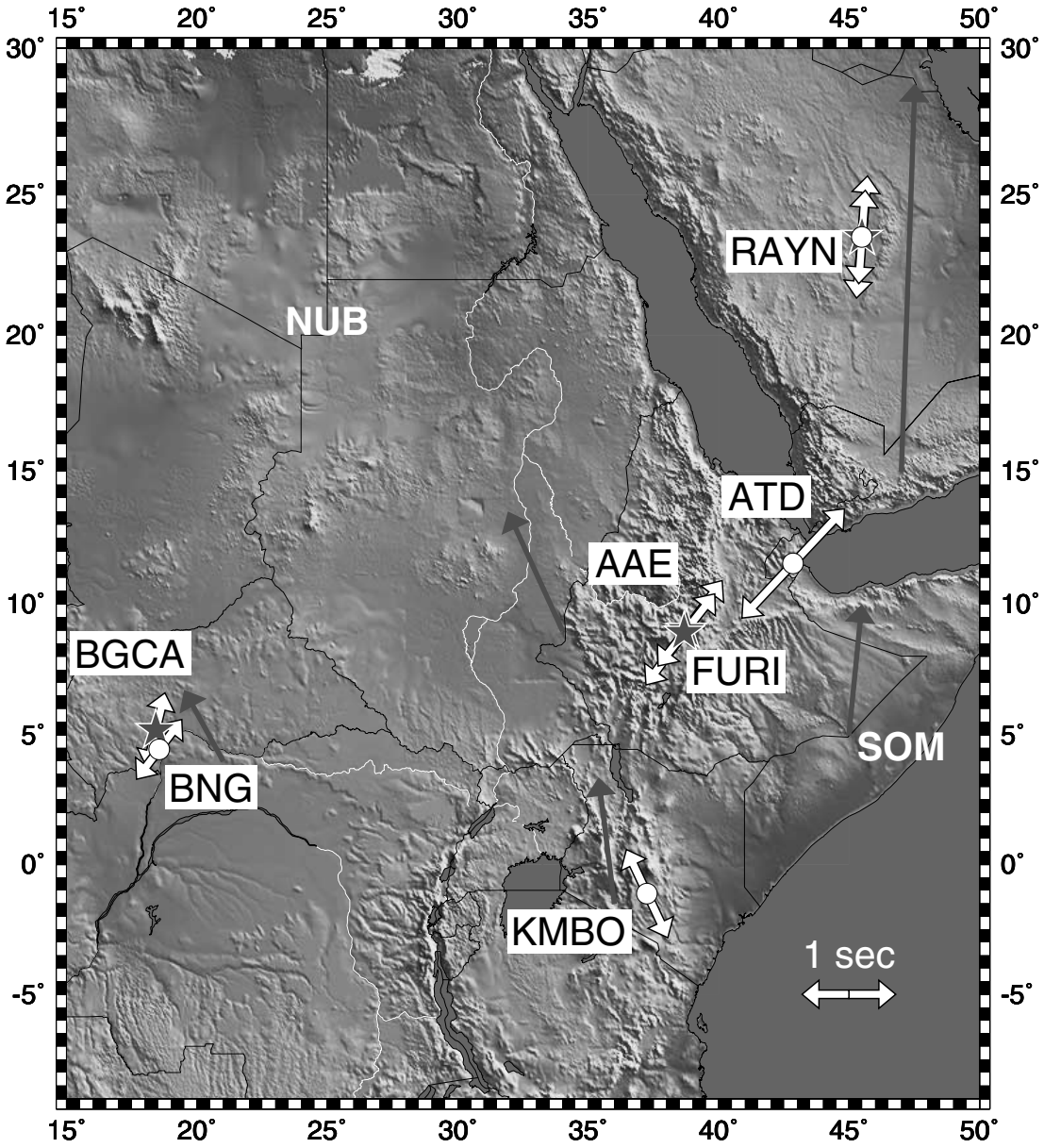

Figure 1. Topographic map of Africa and Arabia showing mean *SKS*-splitting results observed at various IRIS/GSN stations. The white arrows are for the splitting parameters where the direction shows the orientation of the fast shear wave and its length is proportional to the splitting time δt. The black arrows show the absolute plate motions for the Nubia and Somalia plates (NUB and SOM, respectively) (Gripp & Gordon 2002; Eagles *et al.* 2002). As well as the new measurements determined in this study (black stars), we also show *SKS*-splitting results observed at BNG, ATD and RAYN (Barruol & Hoffman 1999; Gao *et al.* 1997; Barruol & Ben-Ismail 2001) (white circles).

The Kaapvaal craton in southern Africa is the world's oldest continental mass. Several shear wave splitting measurements were made in the 1990s (Silver & Chan 1991; Vinnik *et al.* 1995, 1996; Silver 1996). Some authors deduced that the orientation of the seismic anisotropy is closely aligned with the APM direction (Vinnik *et al.* 1996), whilst others argue that it is associated with past tectonic events (Silver 1996). A general north–south fast anisotropy orientation for the whole of the African continent was obtained from azimuthal analysis of the Rayleigh waves by Hadiouche *et al.* (1989) who, also, concluded that the fast direction is consistent with the absolute plate motion. However, there is strong evidence from a more recent experiment in the Kaapvaal craton (Silver *et al.* 2001) that fast *SKS*-polarization directions systematically follow the trend of fossil anisotropy and do not align with the APM direction.

The EAR has long been considered a classic area to study the early phases of continental breakup. Rift propagation is believed to run parallel to old orogenic fabric (Vauchez & Barruol 1996; Vauchez *et al.* 1997, 2000; Tommasi & Vauchez 2001). *SKS*-splitting measurements from the EAR show splitting delay times (δt) of 1.0 and 1.6 s in Kenya and Djibouti, respectively, and a fast shear wave polarization (ϕ) subparallel to the rift trend (Gao *et al.* 1997, 1999; Barruol & Hoffman 1999; Barruol & Ben-Ismail 2001) (Fig. 1). In general, the fast polarization direction (ϕ) is not parallel to the extension direction in continental rifts (Savage 1999; Tommasi *et al.* 1999). In contrast, at oceanic spreading centres mantle flow orients

olivine crystals in the direction of plate spreading (Hess 1964; Blackman *et al.* 1996; Wolfe & Solomon 1998). The possible sources of rift-parallel fast directions (Vauchez *et al.* 2000) in East Africa are:

(i) pre-rift orogenic fabric,
(ii) lattice preferred orientations (LPO) resulting from hot flowing mantle that aligns olivine *a*-axis in a horizontal direction parallel to the rift,
(iii) rift-parallel vertically-oriented melt pockets in the asthenospheric wedge beneath the rift,
(iv) some combination of the above mechanisms.

The rift in Ethiopia separates the Nubia Plate to the NW from the Somalia Plate to the SE (Fig. 1). Rifting here is unique as the northern Ethiopian rift marks the transition from continental rifting to oceanic rifting in Afar. No shear wave splitting analyses have as yet been published in this part of the EAR. We analyse shear wave splitting from *SKS* and *SKKS* phases at the IRIS/GSN (Incorporated Research Institution for Seismology/Global Seismic Network) broad-band stations of FURI and AAE, located on the margin of the main Ethiopian rift near Addis Ababa. We compare the results with previous observations on the African continent and our new measurements at the broad-band stations BGCA (Central Africa Republic) and RAYN (Saudi Arabia) on stable tectonic provinces. Previous *SKS* measurements in Saudi Arabia (Wolfe *et al.* 1999) are augmented at RAYN using more events. The other objectives of this study are:

(i) To summarize the shear wave splitting parameters for the East African rift and surrounding region, to better understand the role of the asthenosphere and lithosphere in the transition from continental rifting in the East African rift to oceanic rifting in Afar.
(ii) To determine receiver functions at the Ethiopian stations to control the possible depth extent of anisotropy.
(iii) To develop self-consistent models to explain the anisotropy.

2 DATA AND METHODS

2.1 Shear wave splitting

The data for *SKS*-splitting measurements in this study consist of three component digital data at four broad-band stations (AAE, FURI, BGCA, RAYN) for earthquakes of magnitude m_b 5.6 to 8.2 in the epicentral distance range 85°–130°. AAE served as an IRIS/GSN station before 1997 and was then replaced by the broad-band station FURI, 20 km south of Addis Ababa. A total of 81 splitting measurements with non-null solutions are analysed for all four stations (Table 1). The African continent is ideally placed to study *SKS* and *SKKS* splitting from earthquakes in circum-Pacific subduction zones, and, to a lesser extent, events from Central and South America. Seismograms were consistently Butterworth band-pass filtered in the range 0.01–0.3 Hz to ensure that variations in splitting parameter estimates are not frequency-dependent.

Shear wave splitting in *SKS* and *SKKS* was measured using the methodology of Silver & Chan (1991). The approach estimates the time separation between the fast and slow shear waves (δt) and the polarization angle of the fast shear wave (ϕ) by finding an inverse splitting operator that best linearizes the particle motion. Elliptical particle motion, and energy observed on the transverse component of the *SKS*/*SKKS* phase, can be diagnostic of shear wave splitting caused by propagation through an anisotropic mantle beneath the recording site. A grid search is employed to find the combination of splitting parameters, ϕ and δt, that best linearizes the particle motion rather than simply minimizing the energy on the transverse component.

Table 1. Table of *SKS*-splitting parameter results. The superscripts 1, 2 and 3 represent Barruol & Hoffman (1999), Barruol & Ben-Ismail (2001) and Wolfe *et al.* (1999), respectively.

Station	δt	Std dev.	ϕ	Std dev.	No. of events
RAYN	1.31	0.05	5	1	20
RAYN[3]	1.01	0.1	4	2	1
ATD[1]	1.6	0.05	43	4	33
FURI	1.38	0.03	36	1	32
AAE	1.00	0.04	38	2	13
KMBO[2]	1.04	0.09	155	4	9
BGCA	0.82	0.03	14	1	16
BNG[1]	0.8	0.08	37	2	30

For each station, we have made individual measurements on all available waveforms with sufficiently clear and isolated *SKS* and *SKKS* phases. The resulting estimates of ϕ and δt for each station (Table 1) were made from weighted averages of the individual observations for the respective number of earthquakes. Fig. 2 illustrates the procedure for an event recorded at FURI for an earthquake of magnitude M_w 7.0 in the region of Bonin Island. To assess the consistency of the splitting parameters we plot them against back-azimuths (Figs 3a and b). Azimuthal variation would indicate depth-varying anisotropy and/or a tilted anisotropy symmetry axis (Levin & Park 1997). Although there is some scatter in the backazimuth variation, a single-layer anisotropic model with a horizontal symmetry axis can explain the observations at FURI (Fig. 3b).

2.2 Receiver functions

There is little information about crust and upper-mantle structure under AAE and FURI. Receiver functions were studied to estimate the thickness of the crust and lithosphere beneath these stations and to help control models of anisotropy depth distribution. Using the source equalization approach (Langston 1979; Ammon 1991), the source, distant path effects and the instrument response can be removed from teleseismic *P* waveforms by deconvolving the vertical from the horizontal components. The source-equalized teleseismic waveform is called the receiver function and is most sensitive to the *P*-to-*S* conversions from structures beneath the recording site (Owens *et al.* 1984). The use of receiver functions to determine crustal structure beneath a three-component broad-band seismograph is now a well-established technique. The amplitudes, arrival times and polarity of the *Ps* conversions can be modelled to provide constraints on the Moho depth and underlying shear wave velocity structure.

In this paper, we model the stacked radial receiver function (Fig. 4) at the FURI broad-band seismic station. There is a noticeable time lag in the arrival of the apparent direct *P* wave. This has been successfully modelled as a marked velocity contrast between shallow low-velocity volcanics and sediments, and underlying basement rock (Owens & Crosson 1988; Cassidy 1992). Except for events with backazimuths aligned with the axis of the main Ethiopian rift, the *Ps* conversions at the Moho are clearly observed with good azimuthal coverage (Fig. 4). The variation in the receiver functions with azimuth and distance (40° to 60°) were such that they could be stacked to increase signal-to-noise ratio (Fig. 4). A distinct low-frequency secondary *Ps* conversion from a deeper mantle interface arrives at approximately 9.5 s after the apparent direct *P*. It is observed on both the individual and stacked radial receiver functions (Fig. 4c).

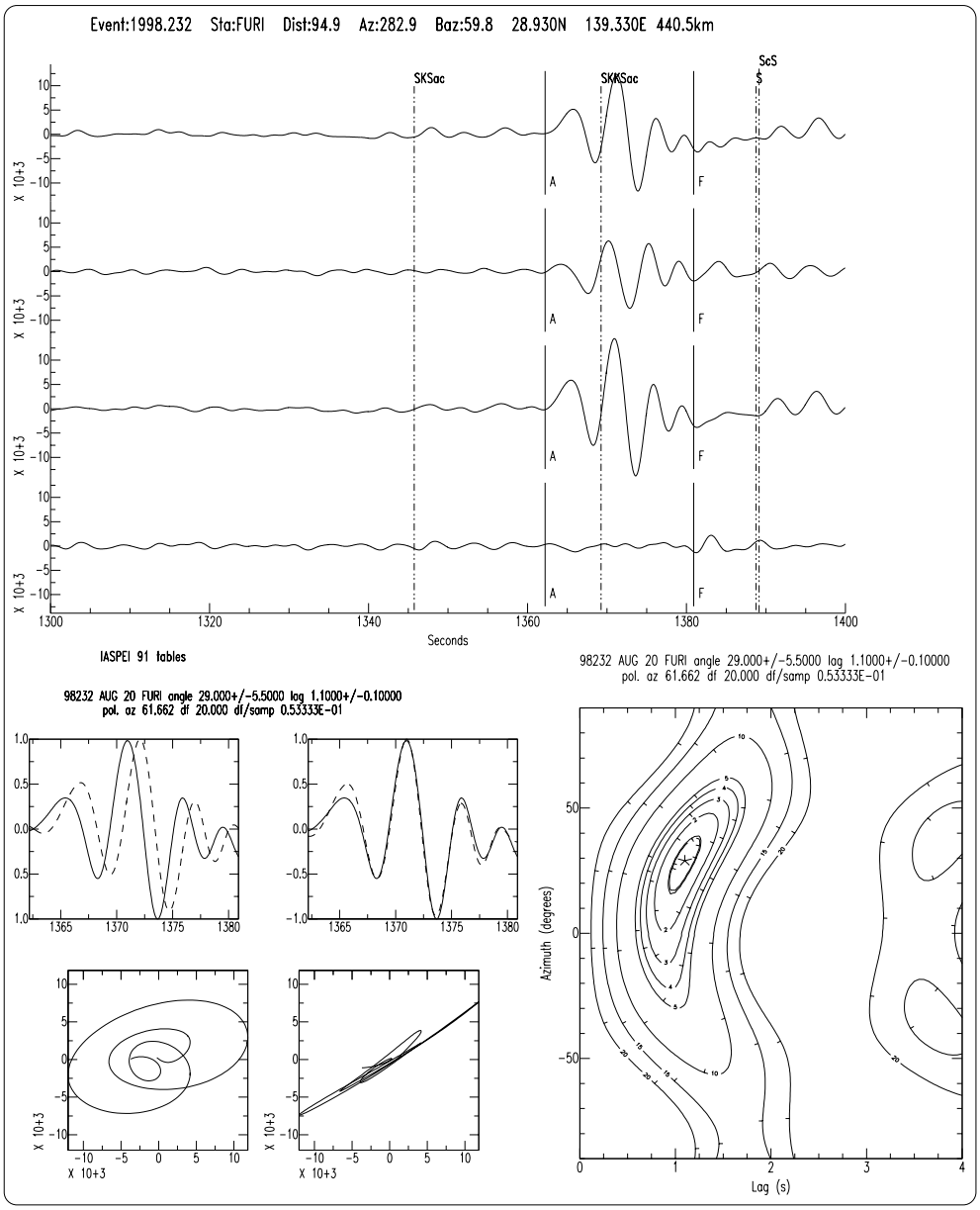

Figure 2. *SKS*-splitting analysis for an event in the region of Bonin Island on 1998 August 20, recorded at station FURI. Predicted arrival times from IASPEI 91 tables for *SKS* and related phases are displayed, also. Note that *SKS* is an exceptionally late arrival. Upper panel: (top two traces) original transverse and radial components; (bottom two traces) transverse and radial components after anisotropy correction. Note the removal of transverse component *SKS* energy in the corrected seismogram. Lower left panel: (top) superposition of fast (ϕ direction) and slow ($\phi + 90^\circ$) shear wave. Uncorrected waveforms shown on the left and corrected waveforms on the right; (bottom) *SKS*-particle motion, uncorrected (left) and corrected (right). Corrections are made using the estimated values of (ϕ and δt). Lower right panel: contour plot of $E_t(\phi\ ,\ \delta t)$. Minimum value (best splitting parameters) marked with an asterix. Contours show 95 per cent confidence region (marked with double contour) and multiples of that contour level.

Receiver functions estimated at AAE are very similar to those at FURI, approximately 20 km away, implying that the velocity structure beneath the western rift margin does not have a dramatic spatial variation.

Forward modelling (reflectivity) of the stacked radial receiver-function at FURI is performed to minimize the difference between the observed and theoretical radial receiver functions. A simple initial crustal velocity-model from Berckhemer *et al.* (1975) was assumed. The results of this inversion are shown in Fig. 5.

3 RESULTS AND DISCUSSION

Table 1 and Fig. 1 summarize our results and those of others (Gao *et al.* 1997; Barruol & Hoffman 1999; Barruol & Ben-Ismail 2001; Wolfe *et al.* 1999). Average splitting values are shown as white arrows on Fig. 1. Black arrows show absolute plate motion (Gripp & Gordon 2002; Eagles *et al.* 2002); note that Africa is nearly stationary in this reference frame and that it is split into the Nubia and Somalia plates (Chu & Gordon 1998; Eagles *et al.* 2002). The polarization angle (ϕ) measured at African stations shows no

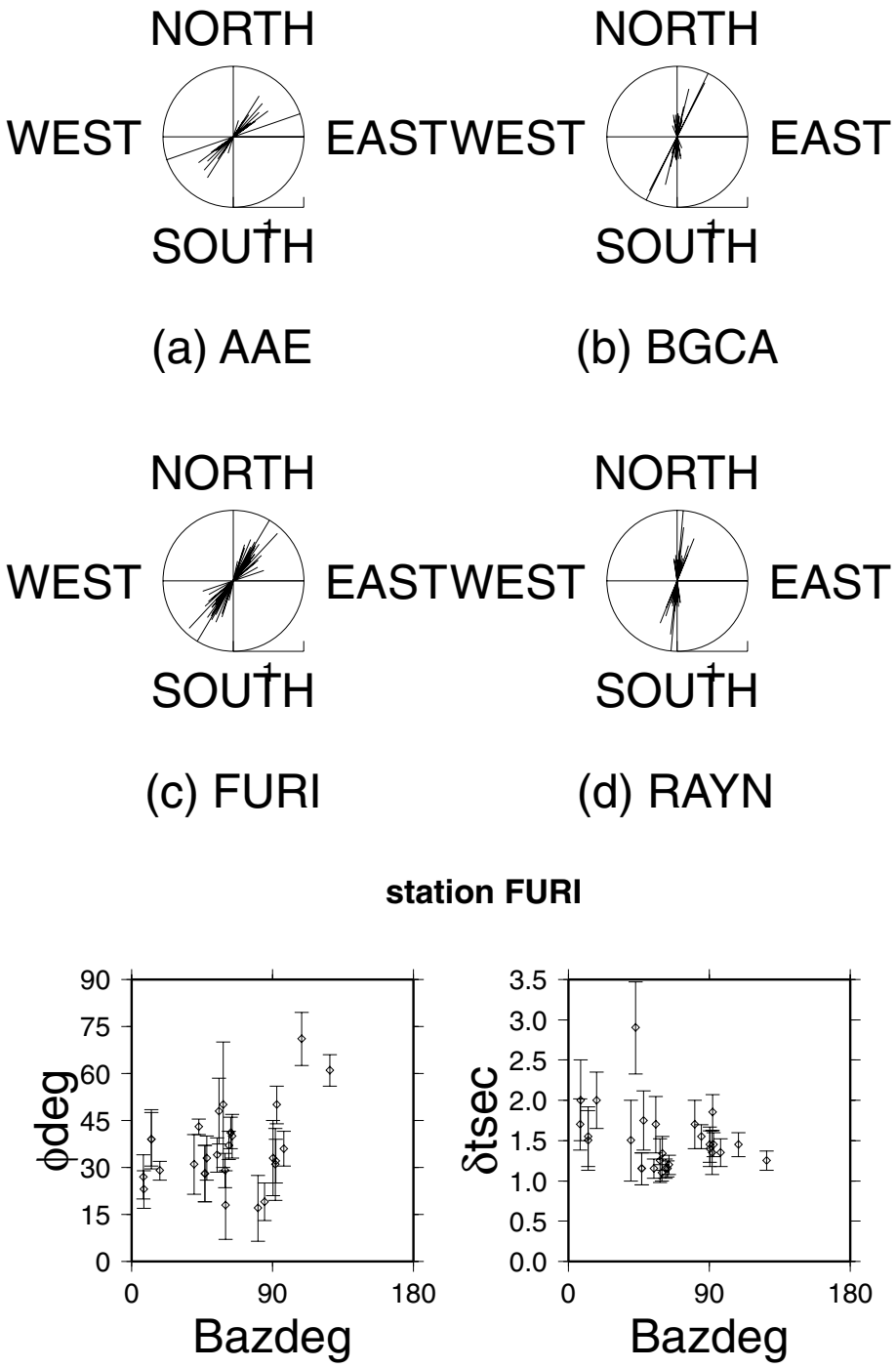

Figure 3. (a) Summary of splitting measurements at each station considered in this study as polar diagrams where the lines in each diagram represent ϕ (the azimuth of the fast split shear wave) and their lengths are proportional to the delay times δt. (b) Anisotropy parameters (ϕ, δt) plotted as a function of earthquake backazimuths estimated at station FURI. Error bars are 1σ uncertainties.

correspondence with APM. In contrast, the station RAYN situated on the fast-moving Arabian Plate shows a fast polarization (ϕ) aligned with the APM. The splitting delay increases in magnitude moving northwards along the East African rift and the polarization of the fast shear wave parallels the trend of the rift. Measurements of Gao *et al.* (1997) for temporary stations deployed in Kenya parallel those shown at KMBO (Barruol & Ben-Ismail 2001).

There is little evidence for multi-layer anisotropy or anisotropy with a dipping symmetry axis. Fig. 3(b) shows no obvious dependency of splitting parameters with backazimuth at FURI.

The general pattern of present-day surface plate motion in the EARS can be influenced by the interaction of ridge push forces from the mid-ocean ridges and mantle convection/upwelling beneath it (Forsyth & Uyeda 1975; Lithgow-Bertelloni & Silver 1998). As a result, the mechanics of rifting in East Africa are probably complex

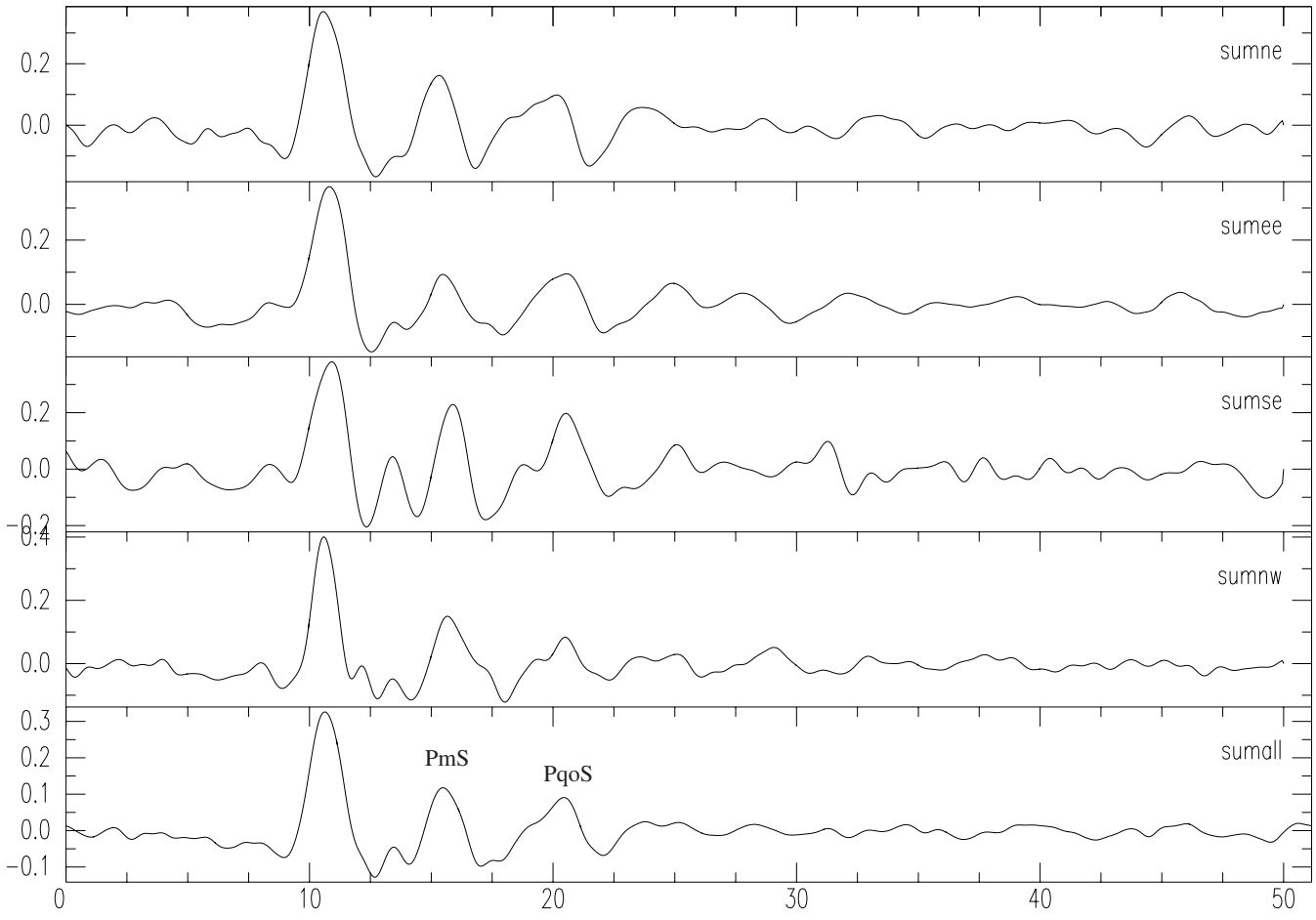

Figure 4. Stacked radial-receiver functions at FURI for northeasterly (sumne), easterly (sumee), southeasterly (sumse), northwesterly (sumnw) and total stack (sumall). PmS – P-wave to S-wave conversion at Moho. PqoS – P-wave to S-wave conversion at 90 km depth.

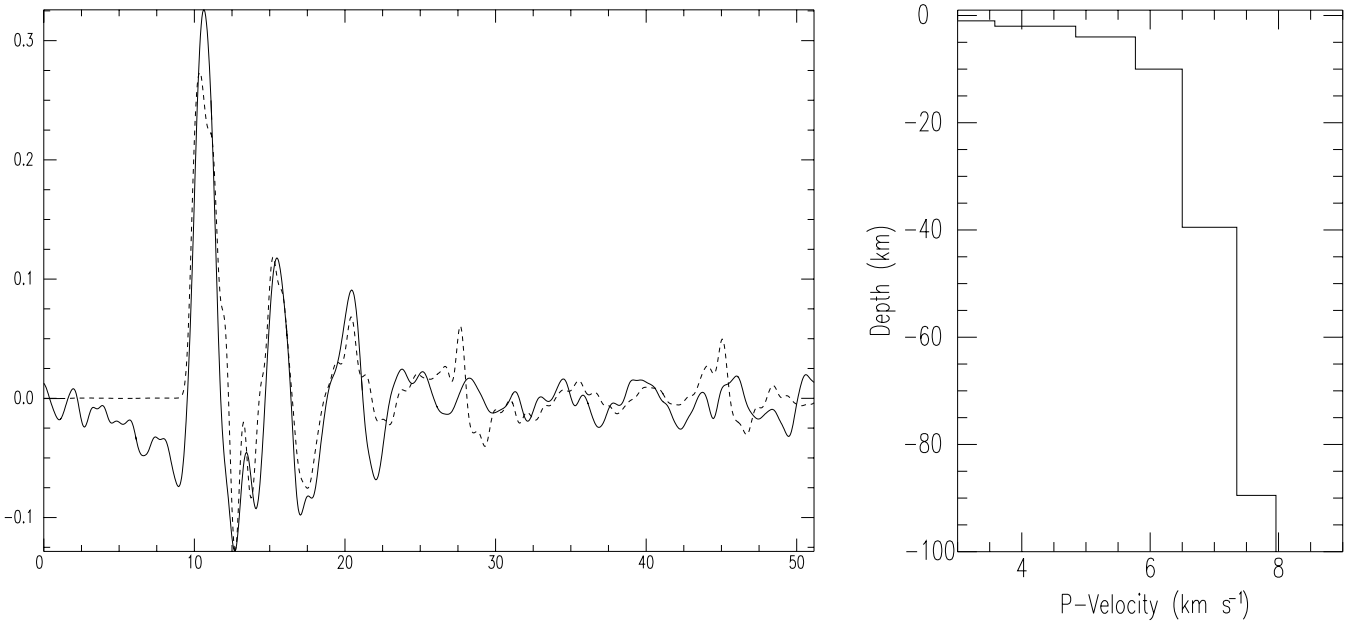

Figure 5. (a) Comparison of the total stack and model radial receiver functions. (b) Preferred shear wave velocity model at FURI from inversion of total stack receiver functions. It illustrates the results of a linearized inversion using a simple seven-layer crust and upper mantle. The model has an *ca* 40 km thick crust, compatible with the refraction results of Berckhemer *et al.* (1975), however, it shows an *ca* 50 km layer below the Moho, also, with anomalous upper-mantle velocities (*ca Vp* 7.4 km s^{-1}; *ca Vs* 4.2 km s^{-1}.

and cannot be explained by a homogeneous lithospheric extension direction as proposed by McKenzie (1978). Seismic tomographic studies suggest the whole lithosphere has been split during rifting processes (Nicolas *et al.*, 1994). Continental breakup in rift zones may occur through a reactivation of the tectonic fabric developed in the lithosphere and mantle during previous orogenic events (Vauchez & Barruol 1996; Tommasi & Vauchez 2001; Collins & Windley 2002). Numerical models (Tommasi *et al.* 1999) suggest that the pre-existing olivine LPO (lattice preferred orientation) tends to be reactivated in trans-tension, a deformation regime that combines strike-slip motion and extension parallel and orthogonal to the rift axis, respectively. There is evidence for oblique deformation in East Africa (Abbate *et al.* 1995; Lepine & Hirn 1992; Ayele 2000) supporting the trans-tension argument. This deformation regime would result in a composite preferred orientation of olivine *a*-axis orientation significantly oblique to the trend of the rift. Such a result is seen across the Dead Sea rift (Rümpker *et al.* 2003). The homogeneous extension model requires the anisotropic response or the olivine *a*-axis to be parallel to the extension direction, however, observation shows that this is not the general rule in all rift systems and does not apply to the East African rift (Gao *et al.* 1997).

Pre-rift deformation, asthenospheric flow and oriented melt pockets are all a possible source of anisotropy beneath rift zones (Vauchez *et al.* 2000). Although we cannot rule out the possibility of fossil anisotropy outside of the rift where asthenosphere upwelling and magmatism is relatively minimal, the ϕ directions and δt values along the EARS seem to favour rift-parallel asthenospheric flow or melt-filled pockets aligned rift parallel, as possible sources of anisotropy (Gao *et al.* 1999; Vauchez *et al.* 1999). From the ϕ orientation and northward increase in δt along the EAR, the observed anisotropy parameters have more to do with the current state of rifting processes influenced by the asthenospheric flow and magmatism, than the fossil anisotropy.

The disparity between ϕ and APM direction at BGCA in Central Africa further implies that continental plates deform coherently with the mantle (Silver & Chan 1991; Silver 1996). A recent earthquake

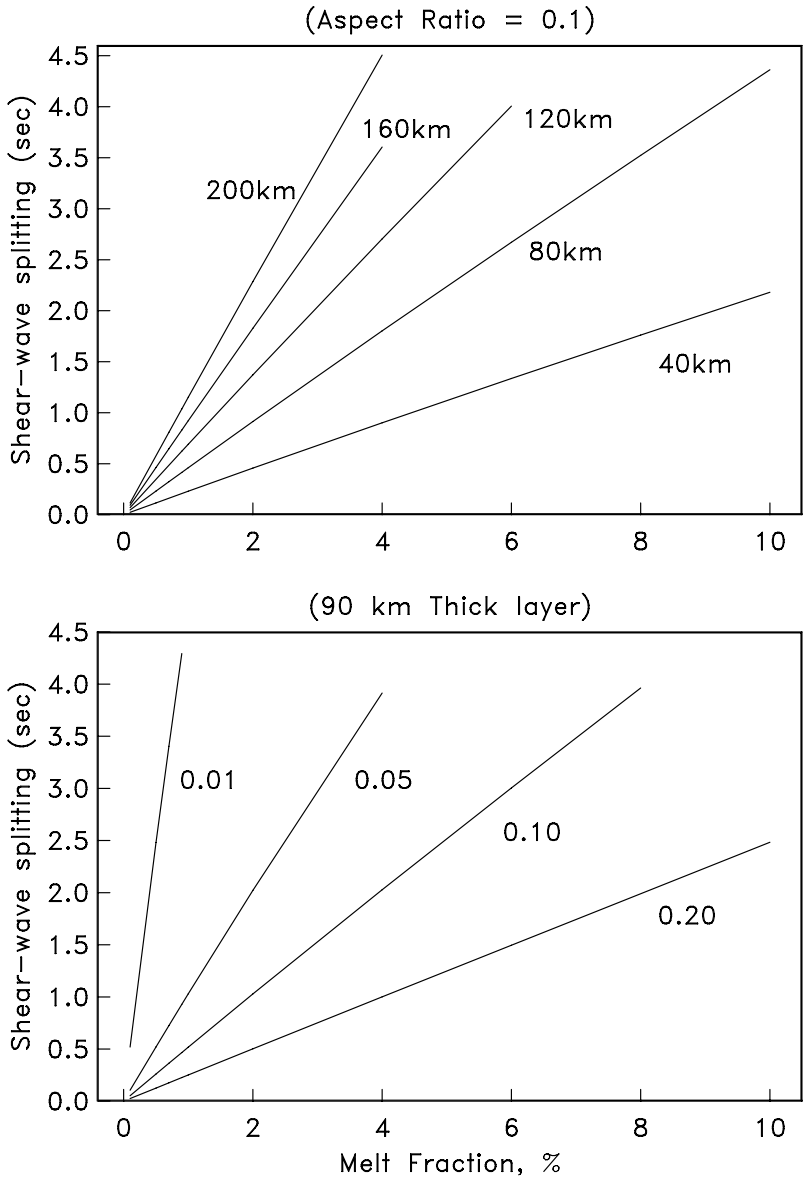

Figure 6. (a) Shear wave splitting delay versus percentage melt fraction for layer thicknesses between 40 and 200 km. The melt is assumed to be present in vertically oriented ellipsoidal cracks with an aspect ratio of 0.1. (b) Shear wave splitting delay versus percentage melt fraction showing the effect of varying the crack aspect ratio for a 90 km thick layer.

source mechanism study in the Congo basin (Ayele 2002) shows that the area is under compressive stress. The *P*-axes of the stress orientation resulting from the E–W contraction nearly parallels the ϕ direction at BGCA, which is the case in typical transpression regions. The anisotropy is predominantly the result of vertically coherent deformation rather than simple asthenospheric flow. This is further supported by evidence for a mantle root that exhibits high shear wave velocity anomalies down to a depth of 250 km beneath the this part of the Nubia Plate (Ritsema & Van Heijst 2000).

The receiver-function result at FURI implies a crustal thickness beneath FURI of 40 km, consistent with previous refraction results (Berckhemer *et al.* 1975), however, the model, also, shows a 50 km thick layer below the Moho with anomalously slow upper-mantle velocity ($V_p = 7.4$ km s^{-1} and $V_s = 4.2$ km s^{-1}), suggesting possibly altered lithospheric material. From Rayleigh wave dispersion, Knox *et al.* (1999) inferred that the uppermost mantle beneath Afar and the northern Ethiopian rift is characterized by a 100 km thick lithosphere overlying an asthenosphere interpreted as having 1–4 per cent partial melt. This result implies that the interface at 90 km depth, found from the FURI receiver-function analysis, could represent the lithosphere/asthenosphere boundary. An interface near a depth of 90 km has been interpreted elsewhere at the Hales discontinuity (e.g. Levin & Park 2000). Its observation is intermittent and its cause unclear.

If the asthenosphere does not contribute significantly to the *SKS*-splitting delay under FURI we have to explain 1.4 s of delay in the top 90 km. Fig. 6(a) shows splitting delays produced by different percentages of vertically-oriented ellipsoidal partial melt-filled cracks for various layer thicknesses. The effective medium theory used in this modelling is that of Tandon & Weng (1984) (see also Kendall 2000). An aspect ratio of 0.1 has been assumed. Fig. 6(b) shows the effect of crack geometry on the relationship between splitting delay and melt fraction. A layer thickness of 90 km has been assumed. $A < 1$ per cent volume fraction of melt aligned in thin vertical ellipsoidal pockets generates sufficient splitting to explain the data. Higher splitting magnitudes in the north can be explained by the higher melt production. Alternatively, anisotropy may be the result of an increase in olivine alignment parallel to the ridge axis in the asthenosphere, as material flows laterally to fill the gap caused by lithospheric extension (Vauchez *et al.* 2000). This model would perhaps imply there should be a region of vertical upwelling mantle somewhere along the rift trend. Such an upwelling would orient the olivine *a*-axes vertically and, hence, produce less splitting (Blackman *et al.* 1996).

4 CONCLUSIONS

Seismological stations on or near the EAR show polarization of the fast shear wave (ϕ) aligned parallel to the rift axis; there is no correlation of ϕ with APM direction. The magnitude of splitting (δt) increases northwards from Kenya (1.0 s) to Ethiopia (1.4 s) to Djibouti (1.6 s). This may reflect the more enhanced role of partial melt in regions of incipient ocean rifting. Less splitting (δt) is observed beneath the cratonic parts of Africa. BGCA in central African shows splitting parallel to the inferred direction of transpression and not the APM direction.

The splitting results at FURI ($\delta t = 1.38 + 0.03$ s, $\phi = 36^\circ + 1$) show a consistency of δt and ϕ with respect to backazimuth, suggesting a single simple anisotropic layer beneath the stations. Preliminary receiver-function analysis at FURI, near Addis Ababa supports refraction experiment evidence of a thick crust close to the rift (*ca* 40 km); there is, also, evidence for a *ca* 50 km thick layer of anomalously slow lithospheric material (*ca Vp* 7.4 km s^{-1}) below the crust.

Our interpretation is that the anisotropy at FURI is the result of aligned melt in the upper 90 km of the lithosphere. $A < 1$ per cent volume fraction of melt aligned in vertical ellipsoidal pockets generates sufficient splitting to explain the data. Further support for this model comes from the fact that the northward increase in δt between FURI and Djibouti correlates with increased surface magmatism toward Djibouti. Alternatively, the anisotropy may be the result of alignment of olivine parallel to the ridge axis, as material flows to fill the gap caused by lithospheric extension. Assuming a uniform magnitude of anisotropy, this would suggest a northward-thickening anisotropic layer beneath the rift and/or an increase in strain that enhances the degree of olivine alignment. Whatever the mechanism, it appears that the anisotropy is sensitive to the transition from continental to oceanic rifting in the northern Ethiopian rift. Our results have motivated models for future experiments to test (e.g. the EAGLE experiment, Maguire *et al.* 2003).

ACKNOWLEDGMENTS

AA thanks the UNESCO/ICSU/TWAS short-term fellowship programme in the basic sciences for financial support. G. Barruol and R. Russo are thanked for reviews that improved the manuscript.

REFERENCES

Abbate, E., Passerini, P. & Zan, L., 1995. Strike-slip faults in a rift area: a transect in the Afar triangle, East Africa, *Tectonophysics,* **241,** 67–97.

Ammon, C.J., 1991. The isolation of receiver effects from teleseismic P waveforms, *Bull. seism. Soc. Am.,* **81,** 2504–2510.

Ayele, A., 2000. Normal left-oblique fault mechanisms as indication of sinistral deformation between the Nubia and Somalia plates in the Main Ethiopian Rift, *J. Afric. Earth Sci.,* **31,** 359–367.

Ayele, A., 2002. Active compressional tectonics in central Africa and implications for plate tectonic models: evidence from fault mechanism studies of the 1998 earthquakes in the Congo Basin, *J. Afric. Earth Sci.,* **35,** 45–50.

Barruol, G. & Ben-Ismail, W., 2001. Upper mantle anisotropy beneath the African IRIS and GEOSCOPE stations, *Geophys. J. Int.,* **146,** 549–561.

Barruol, G. & Hoffman, R., 1999. Seismic anisotropy beneath the Geoscope stations from SKS splitting, *J. geophys. Res.,* **104,** 10 757–10 774.

Berckhemer, H.*et al.,* 1975. Afar Depression of Ethiopia, in *Schweizerbart*, Vol. 1, pp. 89–107, eds Pilger, A. & Rösler, A., E. Schweizerbart'sche Verlagsbuchhandlung, Science Publishers, Stuttgart.

Blackman, D. K., Kendall, J.-M., Dawson, P., Wenk, H.-R., Boyce, D. & Phipps Morgan, J., 1996. Teleseismic imaging of subaxial flow at mid-ocean ridges: travel-time effects of anisotropic mineral texture in the mantle, *Geophys. J. Int.,* **127,** 415–426.

Cara, M. & Leveque, J.J., 1988. Anisotropy of the asthenosphere: the higher mode data of the Pacific revisited, *Geophys. Res. Lett.,* **15,** 205–208.

Cassidy, J.F., 1992. Numerical exeriments in broadband receiver function analysis, *Bull. seism. Soc. Am.,* **82,** 1453–1474.

Chu, D. & Gordon, R., 1998. Evidence for motion between Nubia and Somalia along the Southwest Indian Ridge, *Nature,* **398**, no. 6722, 64–67.

Collins, A.S. & Windley, B.F., 2002. The tectonic evolution of central and northern Madagascar and its place in the final assembly of Gondawana, *J. Geol.,* **110,** 325–339.

Eagles, G., Gloaguen, R. & Ebinger, C., 2002. Kinematics of the Danakil microplate., *Earth planet Sci. Lett.,* **203,** 607–620.

Fischer, K.M. & Wiens, D.A., 1996. The depth distribution of mantle anisotropy beneath the Tonga subduction zone, *Earth planet. Sci. Lett.,* **142,** 253–260.

Forsyth, D. & Uyeda, S., 1975. On the relative importance of the driving forces of plate motions, *Geophys. J. R. astr. Soc.,* **43,** 163–200.

Friederich, W. & Huang, Z.-X., 1996. Evidence for upper mantle anisotropy beneath southern Germany from Love and Rayleigh wave dispersion, *Geophys. Res. Lett.,* **23,** 1135–1138.

Gao, S. *et al.*, 1997. SKS splitting beneath continental rift zones, *J. geophys. Res,* **102,** 22 781–22 797.

Gao, S. *et al.*, 1999. Reply., *J. geophys. Res.,* **104,** 10 791–10 794.

Gripp, A.E. & Gordon, R.G., 2002. Young tracks of hotspots and current plate velocities, *Geophys. J. Int.,* **150,** 321–361.

Hadiouche, O., Jobert, N. & Montagner, J.P., 1989. Anisotropy of the African Continent inferred from surface waves, *Phys. Earth planet. Int.,* **58,** 61–81.

Hess, H. H., 1964. Seismic anisotropy in the uppermost mantle under oceans, *Nature,* **203,** 629–631.

Kendall, J.M., 2000. Seismic anisotropy in the boundary layers of the Mantle, in *Earth's Deep Interior: Mineral Physics and Tomography from the Atomic to the Global Scale*, Geophys. Monogr. Ser. 117, pp. 133–159, eds Shun-ichiro Karato *et al.* AGU, Washington.

Knox, R., Nyblade, A. & Langston, C., 1999. Upper mantle S velocities beneath Afar and western Saudi Arabia from Rayleigh wave dispersion, *Geophys. Res. Lett.,* **25,** 4233–4236.

Langston, C.A., 1979. Structure under mount Rainier, Washington, inferred from teleseismic body waves, *J. geophys. Res.,* **84,** 4749–4762.

Lepine, J.-C. & Hirn, A., 1992. Seismotectonics in the republic of Djibouti, linking the Afar Depression and the Gulf of Aden, *Tectonophysics,* **209,** 65–86.

Levin, V. & Park, J., 1997. P-SH conversions in a flat-layered medium with anisotropy of arbitrary orientations, *Geophys. J. Int.,* **131,** 253–266.

Levin, V. & Park, J., 2000. Shear zones in the Proterozoic lithosphere of the Arabian Shield and the nature of the Hales discontinuity, *Tectonophysics,* **323,** 131–148.

Lithgow-Bertelloni, C. & Silver, P.G., 1998. Dynamic topography, plate driving forces and the African superswell, *Nature,* **395,** 269–272.

Maguire, P. *et al.*, 2003. Geophysical project in Ethiopia studies continental break-up, *EOS, Trans. Am. geophys. Un.,* **84**, 35, 337, 342–343.

McKenzie, D., 1978. Some remarks on the development of sedimentary basins, *Earth planet. Sci. Lett.,* **40,** 25–32.

Nicolas, A., Achauer, U. & Daignieres, M., 1994. Rift initiation by lithospheric rupture, *Earth Planet. Sci. Lett.,* **123,** 281–298.

Nicolas, A. & Christensen, N., 1987. Formation of anisotropy in upper mantle peridotites—A review, in *Composition, Structure and Dynamics of the Lithosphere-Asthenosphere System*, pp. 11–123, eds Fuchs, K. & Froidevaux, C., AGU, Washington, DC.

Owens, T.J. & Crosson, R.S., 1988. Shallow structure effects on broadband teleseismic P waveforms, *Bull. seism. Soc. Am.,* **78,** 96–108.

Owens, T.J., Zandt, G. & Taylor, S.R., 1984. Seismic evidence for ancient rift beneath the Cumberland plateau, Tennessee: A detailed analysis of broadband teleseismic P waveforms, *J. geophys. Res.,* **89,** 7783–7795.

Ritsema, J. & Van Heijst, H., 2000. New seismic model of the upper mantle beneath Africa, *Geology,* **28,** 63–66.

Rümpker, G., Ryberg, T., Bock, G. & DESERT Seismology group, 2003. Boundary-layer mantle flow under the Dead Sea transform fault inferred from seismic anisotropy, *Nature,* **425,** 497–501.

Savage, M.K., 1999. Seismic anisotropy and mantle deformation: what have we learned from shear wave splitting, *Rev. Geophys.,* **37,** 65–106.

Silver, P.G., 1996. Seismic anisotropy beneath the continents, *Ann. Rev. Earth planet. Sci.,* **24,** 385–432.

Silver, P. & Chan, W., 1991. Shear wave Splitting and Subcontinental Mantle Deformation, *J. geophys. Res.,* **96,** 16 429–16 454.

Silver, P.G., Gao, S.S., Liu, K.H. & the Kaapvaal Seismic Group, 2001. Mantle deformation beneath southern Africa, *Geophys. Res. Lett.,* **28,** 2493–2496.

Tandon, G.P. & Weng, G.J., 1984. The effect of aspect ratio of inclusions on the elastic properties of unidirectionally aligned composites, *Polymer Composites,* **5,** 327–333.

Tommasi, A. & Vauchez, A., 2001. Continental rifting parallel to ancient collisional belts: an effect of the mechanical anisotropy of the lithospheric mantle, *Earth planet Sci. Lett.,* **185,** 199–210.

Tommasi, A., Tikoff, B. & Vauchez, A., 1999. Upper mantle tectonics: three-dimensional deformation, olivine crystallographic fabrics and seismic properties, *Earth planet Sci. Lett.,* **168,** 173–186.

Vauchez, A. & Barruol, G., 1996. Shear wave splitting in the Appalachians and the Pyrenees: importance of the inherited tectonic fabric of the lithosphere, *Phys. Earth planet. Int.,* **95,** 127–138.

Vauchez, A., Barruol, G. & Tommasi, A., 1997. Why do continents break up parallel to ancient orogenic belts?, *TerraNova,* **9,** 62–66.

Vauchez, A., Barruol, G. & Nicolas, A., 1999. Comment on 'SKS splitting beneath continental rift zones' by Gao *et al.*, *J. geophys. Res.,* **104,** 10 787–10 789.

Vauchez, A., Tommasi, A., Barruol, G. & Maumus, J., 2000. Upper mantle deformation and seismic anisotropy in continental rifts, *Phys. Chem. Earth,* **25,** 111–117.

Vinnik, L.P, Green, R.W.E. & Nicolaysen, L.O., 1995. Recent deformation of the deep continental root beneath southern Africa, *Nature,* **375,** 50–52.

Vinnik, L.P., Green, R.W.E. & Nicolaysen, L.O., 1996. Seismic constraints on dynamics of the mantle of the Kaapvaal craton, *Phys. Earth. planet. Int.,* **95,** 139–151.

Wolfe, C.J. & Solomon, S.C., 1998. Shear-wave splitting and implications of mantle flow beneath the MELT region of the East Pacific Rise, *Science,* **280,** 1230–1232.

Wolfe, C.J., Vernon, F.L. & Al-Amri, A., 1999. Shear-wave splitting across western Saudi Arabia: The pattern of upper mantle anisotropy at a Proterozoic shield, *Geophys. Res. Lett.,* **26,** 779–782.